HHS Public Access

Author manuscript

DNA Repair (Amst). Author manuscript; available in PMC 2016 October 01.

Published in final edited form as:

DNA Repair (Amst). 2015 October ; 34: 18–27. doi:10.1016/j.dnarep.2015.07.004.

Preferential retrotransposition in aging yeast mother cells is correlated with increased genome instability

Melissa N. Patterson, **Alison E. Scannapieco**, **Pak Ho Au**, **Savanna Dorsey**, **Catherine A. Royer**, and **Patrick H. Maxwell***

Department of Biological Sciences, Rensselaer Polytechnic Institute, Troy, NY

Abstract

Retrotransposon expression or mobility is increased with age in multiple species and could promote genome instability or altered gene expression during aging. However, it is unclear whether activation of retrotransposons during aging is an indirect result of global changes in chromatin and gene regulation or a result of retrotransposon-specific mechanisms. Retromobility of a marked chromosomal Ty1 retrotransposon in *Saccharomyces cerevisiae* was elevated in mother cells relative to their daughter cells, as determined by magnetic cell sorting of mothers and daughters. Retromobility frequencies in aging mother cells were significantly higher than those predicted by cell age and the rate of mobility in young populations, beginning when mother cells were only several generations old. New Ty1 insertions in aging mothers were more strongly correlated with gross chromosome rearrangements than in young cells and were more often at non-preferred target sites. Mother cells were more likely to have high concentrations and bright foci of Ty1 Gag-GFP than their daughter cells. Levels of extrachromosomal Ty1 cDNA were also significantly higher in aged mother cell populations than their daughter cell populations. These observations are consistent with a retrotransposon-specific mechanism that causes retrotransposition to occur preferentially in yeast mother cells as they begin to age, as opposed to activation by phenotypic changes associated with very old age. These findings will likely be relevant for understanding retrotransposons and aging in many organisms, based on similarities in regulation and consequences of retrotransposition in diverse species.

Keywords

Retrotransposon; replicative aging; *Saccharomyces cerevisiae*; Ty1; chromosome rearrangements; Gag

*Corresponding author: Patrick Maxwell, Rensselaer Polytechnic Institute, CBIS Room 2123, 110 8th Street, Troy, NY 12180, 518-276-2166, maxwep2@rpi.edu.

Conflicts of interest statement

The authors declare that there are no conflicts of interest.

Supplementary Data

Three figures and one table are included as Supplementary Data.

1. Introduction

Retrotransposons are mobile DNA elements that have been recently associated with aging in a variety of organisms. These elements transpose through reverse transcription of their RNA transcripts into DNA copies that are incorporated at new genomic sites [1]. Increased retrotransposon RNA or protein levels have been observed with increased age in *S. cerevisiae* mother cells, *Caenorhabditis elegans* gonads, *Drosophila melanogaster* brain tissue, mouse somatic tissues, and senescent human fibroblasts [2–7]. Reporter genes were used to directly detect elevated insertions of the *gypsy* element in brain tissue from aged *D. melanogaster* and the Ty1 retrotransposon late during the lifespan of nondividing yeast cells [5, 8]. Quantitative PCR (qPCR) has been used to infer increased mobility through increased retrotransposon copy number in aging yeast mother cells, mice, and human cells [3, 4, 6]. These elements can cause mutations, contribute to chromosome rearrangements, produce double-stranded DNA breaks, and alter transcriptional regulation or mRNA splicing of neighboring gene sequences, so their elevated activity may promote aging by causing genome instability and changing gene expression patterns [9–14]. Age-dependent loss of chromatin-based and small RNA-based silencing mechanisms, as well as activation of retrotransposons by reactive oxygen species and DNA damage, may underlie this activation of retrotransposons with age, allowing them to cause genetic damage [15–17].

Many questions remain regarding the relationship between retrotransposons and aging, including whether there is any specific age-related regulation of retrotransposons or whether they are reacting only to global changes in chromatin and other gene regulatory mechanisms [17]. Also, the reliability of estimating levels of retrotransposition using qPCR-based measurements of copy number has been questioned [18], highlighting the importance of directly measuring retrotransposition to formally rule out contributions of other DNA amplification mechanisms or the presence of unincorporated reverse transcripts to copy number changes detected by qPCR. While there is evidence that human *Alu* element expression can contribute to DNA damage in senescent cells [19], evidence that retrotransposition itself is directly contributing to age-dependent genome instability is also needed. The relationship between these elements and aging may be complex, since an earlier report had found retrotransposition to be decreased in primary human fibroblasts as they approached replicative senescence [20], and we have recently reported that retrotransposons can have unexpected positive influences on aging in certain contexts [21].

S. cerevisiae provides an excellent model to address many of these questions. Studies of yeast replicative aging that occurs as mother cells undergo successive rounds of cell division and chronological aging of nondividing cells have provided important insights relevant to aging in a number of species [22]. Ty1 is a well-characterized long terminal repeat (LTR) retrotransposon in *S. cerevisiae*, and mobility frequencies or rates of endogenous Ty1 elements expressed from their native promoters can be easily and quantitatively measured using indicator genes [1, 23, 24]. In this study, potential age-specific regulation of Ty1 retromobility during replicative aging was examined by separating mother and daughter cells through magnetic sorting. Yeast mother cells have higher than predicted levels of new Ty1 insertions, which are more often associated with gross chromosome rearrangements (GCRs) than in young cells, and mother cells have much higher levels of extrachromosomal

Ty1 complementary DNA (cDNA) than their daughters. These results provide strong support for mother cell-specific (or age-specific) regulation of retrotransposition that could contribute to genome instability during replicative aging.

2. Materials and methods

2.1. Yeast strains, media, and plasmids

Yeast strains were grown using standard rich (YPD) or synthetic complete (SC) medium [25]. Strain JC3212, which is a derivative of BY4741 with a chromosomal copy of Ty1*his3AI* [26], was used for most experiments. Strain JC3807 was used for fluorescence fluctuation microscopy through two photon scanning Number & Brightness, and it has the same genotype as JC3212 but also harbors a chromosomal Ty1-*GFP*-3566 element in which *GFP* is fused to the 3′ end of the *TYA1* ORF to produce a Gag-GFP fusion protein [27, 28].

2.2. Isolation of yeast mother cells and determination of cell age

Magnetic cell sorting to separate biotin-labeled mother cells from their daughter cell populations was performed as previously described [29]. Briefly, cells were grown from glycerol stocks on YPD agar at 30°C, and 10^8 cells per collection point were labeled with NHS-LC-biotin (Thermo Scientific) and inoculated into YPD medium at a density of 5×10^6 cells/ml. Labeled cells were magnetically sorted after overnight growth at 20°C using anti-biotin microbeads and MACS LS separation columns (Miltenyi Biotec), and no more than 2×10^9 cells were loaded onto individual columns. At each collection point, portions of the column eluate (mother cells) and flow through (daughter cells) were retained for analyses, and portions of sorted mother cells were inoculated into YPD liquid medium for additional rounds of growth and sorting to increase replicative age. Cell populations grown overnight and washed with buffer in preparation for sorting were stored on ice for up to one hour, and labeled or sorted cells were stored for up to three hours on ice before inoculation into fresh medium in some instances [29]. Bud scars were stained with an Alexa Fluor 488 conjugate of wheat germ agglutinin (WGA, Life Technologies) to determine replicative age of cells. Manual bud scar counts obtained from fluorescence microscopy were plotted versus the geometric means of fluorescence intensity of stained cells measured with a BD LSR II flow cytometer and normalized to unstained controls for three trials to obtain a trend line for calculating cell age [29]. Cell ages for populations were then calculated from normalized geometric mean signals from individual trials using unsorted control populations to verify consistent staining and were averaged for multiple trials in a given set of experiments. Cell viability was determined directly using trypan blue dye exclusion, as previously described [29]. Plating efficiencies were determined from the percent of cells spread onto rich medium that were able to form colonies after incubation at 30°C for five days, and the values reported for mother cells of different ages were normalized to the initial plating efficiencies of the strains.

2.3. Ty1 retromobility rate and frequency

The frequency of His^+ prototroph formation was used to calculate the rate and frequency of retromobility of a chromosomal Ty1*his3AI* element in unsorted or sorted cell populations [30]. Diluted cells were spread onto YPD medium and incubated for up to five days at 30°C

to determine colony-forming units/ml, while appropriate volumes of cells (no more than 10^8 cells per plate) were spread onto SC medium lacking histidine and incubated for up to seven days at 30°C. Retromobility frequencies were calculated as the number of His^+ prototrophs divided by the colony-forming units spread onto selective medium. Seven to ten replicate cultures were inoculated at 5,000 cells/ml and grown for three days to measure initial frequencies for cells grown at 30°C and for fluctuation tests to measure rates of Ty1*his3AI* mobility at 20°C [31]. Rates were calculated using the Ma-Sandri-Sarkar (MSS) maximum likelihood method [32]. Predicted retromobility frequencies for cells of given ages were calculated as described previously using initial frequencies and retromobility rate values [29].

2.4. Adapter and multimer PCR for Ty1*HIS3* insertions

Genomic DNA extracted by glass bead disruption and phenol extraction from His^+ prototrophs from sorted cell populations was used for adapter-mediated PCR to identify genomic DNA flanking the 3′ end of Ty1*HIS3*. Approximately two μg of genomic DNA was digested with combinations of the following blunt-end producing restriction enzymes: EcoRV, HincII, PvuII, SnaBI, and StuI. Digested DNA was purified with the Wizard SV Plus PCR Clean-up Kit (Promega) in a final volume of 50 μl, and six μl was ligated to a DNA adapter (final adapter concentration of 3.75 μM) in a total volume of 10 μl. The adapter was formed by annealing two oligonucleotides: 5′-ACGCTACACGTCGGTCGACTCCACTCGAGCTGACTAGTTGGATCC-3′ and 5′-GGATCCAACTAGTCAG-3′. The shorter oligonucleotide had a 5′-phosphate and a 3′-amine group, the latter of which prevented extension of the shorter strand of the adapter to reduce nonspecific PCR products [33]. One μl of each ligation reaction was amplified by PCR using an adapter-specific primer (5′-ACGCTACACGTCGGTCGACTCCA-3′) and a *HIS3* primer overlapping the splice junction formed after removal of the artificial intron (5′-TCTCCTACTTTCTCCCTTTGCAAACC-3′). One μl of each first round PCR was amplified using a partially nested adapter primer (5′-GACTCCACTCGAGCTGACTAGTTG-3′) and a nested *HIS3* primer (5′-CCTTCGTTTATCTTGCCTGCTC-3′). PCR products were purified with the Wizard SV Plus PCR Clean-up Kit (Promega) and sequenced. Ty1 multimers (tandem Ty1 insertions) were detected by PCR using the *HIS3* splice junction primer and an antisense primer to the *TYA1* region of Ty1 (5′-TGAGGTTAACATTGGTGGTGGTCTG-3′). Control primers to the *BAT1* gene were included in these reactions to verify negative results.

2.5. CHEF gel analysis of chromosome instability

Intact yeast chromosomes were prepared and analyzed using a CHEF Mapper XA Chiller clamped homogeneous electrical field (CHEF) electrophoresis system (Bio-Rad) as previously described, except that gels were run at a 60° angle for 18 h with pulse times of 40–75 sec and then for 8 h with pulse times of 110–130 sec [34].

2.6. Quantification of Ty1*HIS3* and Ty1*his3AI* mRNA

Total yeast RNA was prepared from unsorted, mother cell, and daughter cell populations using the MasterPure Yeast RNA Purification Kit (Epicentre) according to the

manufacturer's instructions and including DNaseI treatment. The PrimeScript 1st Strand cDNA Synthesis Kit (Takara Bio) was used according to the manufacturer's instructions to prepare cDNA and mock (minus reverse transcriptase) samples. PCR products generated with primers hybridizing to *ACT1* (5′-CGAAAGATTCAGAGCCCCAGAAGCT-3′ and 5′-GGAGCCAAAGCGGTGATTTCCT-3′) and spliced *HIS3* (5′-TGGATGAGGCACTTTCCAGAG-3′ and *HIS3* splice junction primer, section 2.4) sequences were generated and quantified using EvaGreen Supermix (Bio-Rad) and a QX200 Droplet Digital PCR (ddPCR) System (Bio-Rad). Total mRNA from the Ty1*his3AI* element (unspliced *his3AI* and spliced *HIS3*) was detected using the first *HIS3* primer listed above, which anneals to a region of *HIS3* absent from the chromosomal *his3Δ1* allele in the strain background, and the primer 5′-CTTTGGTGGAGGGAACATCGTTG-3′. Absolute quantification was performed to determine copies/μl for each target, using triplicate technical replicates, and subtracting the very low signal obtained from mock samples (if any signal from mock samples was detected). Ty1*HIS3* and total Ty1*his3AI* mRNA levels were normalized using *ACT1* mRNA levels, and levels of unspliced Ty1*his3AI* mRNA were determined by subtracting the copies/μl of Ty1*HIS3* from the copies/μl of the total Ty1*his3AI* mRNA.

2.7. Determination of Ty1 Gag-GFP concentration

Yeast strain JC3807 expressing Ty1 Gag-GFP was grown at 20°C in synthetic complete medium lacking adenine and tryptophan (SC – Ade – Trp) to obtain unsorted cell populations or labeled with biotin and used for magnetic sorting (as in section 2.2) to obtain mother and daughter cell populations. Sorted cells were suspended in phosphate buffered saline. Cells were imaged by two photon scanning Number and Brightness (N&B) on agar pads exciting at 930 nm, using 10 mW laser power (Mai Tai fs IR laser, Newport, Spectra-Physics, Santa Clara, CA) at the entrance to the Alba mirror scanning fluorescence fluctuation microscope (ISS, Urbana, IL). Pixel dwell time was set to 40 microseconds, and stacks of 50 20×20 micrometer images of 256×256 pixels were acquired using a 735-LP long-pass dichroic mirror (FF735-Di01) and a 750 nm (750sp-2p) low pass blocking filter and a 542 nm bandpass filter (FF01-530/43-25) in emission (all from Semrock, Rochester, NY). Raw Number and Brightness values were corrected for shot noise contributions by subtracting 1 from the B value to yield true brightness, e, and by dividing the product of N × B by the true brightness (B-1) to yield, n, the true number of molecules in the two-photon point spread function (PSF) as previously described [35].

In dozens of fields of view, hundreds of yeast cells were sized assuming roughly spherical shape and sorted as mothers, buds and daughters. The auto-fluorescent and dark count threshold was found to be 0.6 counts per second per dwell time, and was subtracted from all images prior to calculating N&B. The values of the true number and brightness were calculated on a single cell basis by averaging the values of all the pixels within each cell. Since Ty1 Gag-GFP formed higher order oligomers and even foci, the total concentration is reported in terms of monomeric GFP. For example, if for a given region in a cell the concentration were 100 nM, but the molecular brightness was 10-fold that of GFP, the total concentration is reported as one μM (10 × 100 nM) for that region. We note that for very large foci that diffused as a unit, the brightness values were very large, and since they did

not always come into focus in the z-plane, the concentration values for those cells containing foci represent a lower limit.

2.8. Quantification of Ty1 cDNA

A previously established Southern blot method was used to quantify Ty1 cDNA [36]. Up to two μg of SphI-digested genomic DNA (prepared as for PCR) resolved on 1% agarose gels was transferred under alkaline conditions to Brightstar-plus positively charged nylon membranes (Life Technologies). Blots were hybridized with a radioactively labeled Ty1 DNA probe prepared from a PCR product corresponding to positions 4221–4842 of Ty1-H3 (GenBank accession M18706.1) in NorthernMax hybridization buffer (Life Technologies) at 45°C overnight. Blots were washed four times at a maximum stringency of 0.2X SSC (0.03 M sodium chloride and 0.003 M sodium citrate), 0.1% sodium dodecyl sulfate at 45°C, visualized using a Typhoon Trio+ imager (GE Healthcare) and quantified with ImageQuant 5.1 software. Ty1 cDNA signal was normalized to the average signal for two genomic Ty1 fragments and then to the signal obtained for control unsorted populations grown at 20°C.

2.9. Statistical analysis

Unpaired two-tailed t-tests assuming equal or unequal variance (depending on the data sets) were used to compare mean values and Fisher's exact test was used to compare ratios for significant differences. Levels of significance are given in the figures and text.

3. Results

3.1 Elevated retromobility in mother cells

Potential age-dependent changes in Ty1 retrotransposition in *S. cerevisiae* were investigated using a method to compare observed frequencies of genome instability to predicted frequencies for cells of different replicative ages [29]. Since yeast cells surface-labeled with biotin do not pass the label to their daughters, initial populations of labeled cells grown in liquid cultures were separated from their daughters with anti-biotin magnetic microbeads and magnetic columns [37]. Sorted mother cells were analyzed or grown and sorted again until they underwent a total of up to five rounds of growth and sorting to increase their age. The yeast strain used harbors a chromosomal copy of a Ty1 retrotransposon with the *his3AI* retrotransposition indicator gene [30] enabling quantification of Ty1 retromobility by measuring the frequency of cells gaining the ability to grow in the absence of histidine (His^+ prototroph phenotype) following genomic insertion of a Ty1*HIS3* cDNA produced from the marked element (Fig. S1) [30]. Cell populations were grown at a non-permissive temperature for Ty1 mobility (30°C) prior to biotin labeling and were then grown at a permissive temperature (20°C) for the remainder of each experiment [38, 39]. The average age in cell generations of populations was determined by staining bud scars on cell surfaces at the sites of prior cell divisions with a fluorescent conjugate of WGA and then performing flow cytometry (see section 2.2) [29]. Histograms from flow cytometry of WGA-stained mother and daughter cell populations confirmed that mother cell populations had very little contamination with daughter cells and vice versa (Fig. S2).

Rates of Ty1*his3AI* mobility per cell generation were calculated using the MSS maximum likelihood estimator method and data from standard cultures (unsorted populations) to predict His^+ prototroph frequencies due simply to additional cell generations (Fig. 1A) [32]. An average Ty1*his3AI* mobility at non-permissive temperature of $6.6 \pm 4.9 \times 10^{-9}$ (mean ± standard deviation) calculated from three trials each using ten independent cultures was added to the product of the mean rate value at permissive temperature from seven trials and the number of cell generations to obtain predicted His^+ prototroph frequencies (Fig. 1B). Error bars for these values were generated by substituting the lower and upper bounds of the mean 95% confidence interval for the rate in the formula. His^+ prototroph frequency in mother cells with mean replicative ages of 4.1 or 12 (one or three rounds of overnight growth and sorting, respectively) was 4.2 or 3.9-fold higher than predicted values, but the frequency was not higher than predicted for mother cells with a mean replicative age of 18 (five rounds of growth and sorting) (Fig. 1B). The observed data from six independent trials were compared to all the predicted values obtained by using each of the seven individual rate values (Fig. 1A) to determine that fold increases were significant. The average purity of sorted mother cells based on bud scar staining for populations 4.1, 12, or 18 divisions old was 77 ± 2.4%, 97 ± 1.4%, or 98 ± 1.0%, respectively (mean ± standard deviation). The reduced purity in the youngest mother cell populations likely results from some mother cells completing cell division during the sorting procedure, due to rapid cell divisions in these young mothers, resulting in limited carry over of daughter cells [29]. Control experiments were also performed to determine whether incubation of cells on ice immediately before or after sorting in some trials (see Section 2.2) or the sorting procedure itself could alter Ty1 mobility. No significant differences were seen in Ty1 mobility comparing cell populations immediately before and after sorting, or due to incubations of cells on ice during the protocol (Fig. S3).

The decreased Ty1 mobility frequency in the oldest mother cells correlated with only a modest decrease in average viability, but a large decrease in the average percentage of cells able to form colonies on fresh medium (plating efficiency, Fig. 1C). This decrease in plating efficiency could contribute to a decreased ability to detect insertions in the oldest mother cells, since colony formation on selective medium is required to detect Ty1*his3AI* mobility. Furthermore, the reduction in plating efficiency prevented reliable mobility measurements from being made beyond five rounds of growth and sorting.

Ty1*his3AI* mobility was 2.2 or 2.4-fold higher in the two younger mother cell populations than in their daughters, but was similar between the oldest mother cells and their daughters (Fig. 1D). Since new Ty1*his3AI* insertions that occur in non-dividing cells would be passed on to subsequent daughter cells, the higher mobility in mother cells could indicate that insertions preferentially occur in mother cell genomes during cell division. The absence of mother-daughter asymmetry in the oldest cells could reflect a breakdown in the mechanism responsible for preferential Ty1 insertions in mother cells or the inability of many of the oldest mother cells accumulating insertions to grow when placed onto fresh medium, preventing their detection (Fig. 1C).

3.2 Ty1 insertions in mother cells are correlated with genome instability

The consequences of elevated retromobility as yeast mother cells begin to age depend partly on the sites of the new Ty1 insertions. In young cell populations, Ty1 preferentially integrates at sites of well-positioned nucleosomes flanking tRNA genes and to a lesser extent other RNA polymerase III-transcribed genes (90–94% of insertions), avoids open reading frames (ORFs, 2–5% of insertions), and frequently integrates at sites of flanking well-positioned nucleosomes when near ORFs [40, 41]. DNA sequences flanking the 3′ end of Ty1*HIS3* in His^+ clones from mother cells of different ages were identified using an adapter-mediated PCR protocol [33] with primers specific for the adapter and the splice junction in *HIS3*, to avoid amplification of the original Ty1*his3AI* element. The total set of insertions for all mother populations analyzed included four insertions (5.3% of insertions) in non-preferred targets: three independent insertions in *RDN25*, the 25S rRNA gene, and one in a telomeric region between a Y′ element and an X element (Table 1, see Table S1 for full list of insertions). A large-scale study in young cells identified approximately 94% of insertions specifically within 2 kb of tRNA genes and relatively few insertions at other RNA pol III transcribed genes [41]. In aging mother cells, 80% of insertions (60/75) were near tRNA genes (Table 1), which is significantly lower than the ratio expected if approximately 94% of insertions occurred near tRNA genes (70/75, $p < 0.05$). While only 13% of 275 nuclear tRNA genes annotated in the Saccharomyces Genome Database (www.yeastgenome.org) are within 1000 bp of a DNA replication origin, 23% of insertions near tRNA genes in aging mother cells (14/60) occurred near tRNA genes within 1000 bp of a DNA replication origin. Nearly 11% of total insertions were near the *RDN5* 5S rRNA gene within the rDNA (also transcribed by RNA Pol III), and two of these insertions occurred in the external transcribed spacer region (5′-ETS) of the rDNA locus [42]. Only 2.7% of insertions were nearby ORFs, similar to what was previously observed in young cells [40, 41], but insertions into the rDNA (*RDN5* and *RDN25*) represented 15% of the total sites, which was not expected. These data are consistent with changes in the suitability of particular genomic targets for insertions or changes in Ty1 insertion preferences in mother cells.

The adapter-mediated PCR analysis also identified some tandem (multimeric) Ty1 insertions, which have been found to be more frequent in strains deleted for the *SGS1* or *RRM3* DNA helicase genes or the *RAD27* flap endonuclease gene and have been correlated with GCRs [43–45]. These insertions were not included in Table 1 or Table S1 because the presence of a downstream Ty1 element prevented assignment of the insertions to a specific genomic site. Using PCR primers to the splice junction in *HIS3* and to the 5′ end of Ty1 (Fig. 2A), the fraction of His^+ clones with multimers in unsorted cultures and mother cells 4.1, 12, or 18 generations old was 14%, 23%, 28%, or 13%, respectively (Fig. 2B). These His^+ clones were also analyzed for GCRs by pulse-field gel electrophoresis of intact chromosomes, and shifted, absent, or new bands were scored as GCRs (Fig. 2C and data not shown). Note that very subtle shifts in the migration of chromosomes I, III, VI, and IX (the smallest chromosomes at <500 kb each) could result from insertion of a single Ty1 element (~6 kilobase pairs) and were not scored as GCRs. GCRs were present in 18%, 48%, 46%, or 27% of His^+ clones from the unsorted populations and mother cells 4.1, 12, or 18 cell generations old, respectively (Fig. 2D). In contrast, only one out of 50 total clones (2%) that

were not selected for new Ty1 insertions from these same mother cell populations harbored a GCR (Fig. 2C and data not shown). His^+ clones with multimeric Ty1 insertions were more likely to have GCRs than those without multimeric insertions, but the difference was significant for only two populations because of the smaller sample sizes when only clones with multimers were considered (Fig. 2D).

3.3 Increased Ty1 mobility in aging mother cells is not due to increased abundance of Ty1*HIS3* mRNA

Elevated Ty1*his3AI* mobility in aging mothers could occur if mothers accumulate more spliced Ty1*HIS3* mRNA than young cells. An increase in Ty1 RNA was previously observed in very old mother cells compared to young daughter cells [6]. Levels of spliced Ty1*HIS3* and unspliced Ty1*his3AI* mRNA in reverse-transcribed RNA samples were examined by ddPCR for two mother cell populations early in their lifespan (average ages 7.7 and 8.3), and two mother populations later in their lifespan (average ages 16 and 19) compared to their daughter populations and unsorted young populations. No significant differences were noted between these two age groups of mothers, so the mother and daughter cell data for these populations were combined for comparison. Normalized levels of Ty1*HIS3* and Ty1*his3AI* mRNA were not elevated in aged mothers compared to unsorted young populations (Fig. 3A), indicating that the higher than expected Ty1 mobility in aged mothers is not due to accumulation of Ty1 mRNA. Mother cells did have two-fold more Ty1*HIS3* mRNA than their daughters (Fig. 3A), indicating that asymmetry in Ty1 mRNA accumulation could contribute to differences in retrotransposition between mothers and daughters. The ratio of spliced Ty1*HIS3* to unspliced Ty1*his3AI* was low in all samples (Fig. 3B), consistent with previous observations [30], and indicating that changes in splicing efficiency do not contribute to high Ty1*his3AI* mobility in mother cells.

3.4. Mother cells are more likely to have very high concentrations and foci of Ty1 Gag-GFP

Since Ty1 Gag forms cytoplasmic foci with Ty1 mRNA and also forms virus-like particles (VLPs) in which Ty1 reverse transcription occurs, accumulation of Gag foci in mother cells could also account for high Ty1 retrotransposition in aging mothers. In prior work, Ty1 Gag-mRNA foci were found to be moderately enriched in budding mother cells compared to non-dividing cells [46]. Ty1 Gag-GFP expressed from a chromosomal Ty1 element was imaged in live yeast cells using two photon scanning N&B. This powerful technique extends fluorescence correlation spectroscopy (FCS) to provide 2D spatial variance analysis of fluorescent particles diffusing in live cells [35, 47, 48]. N&B analysis uses the variance in the fluorescence intensity at each pixel of a stack of rapid raster scans to calculate the absolute average number (N) of fluorescent molecules in the two photon excitation volume at each pixel, as well as their molecular brightness (B, in counts per pixel dwell-time per molecule). The absolute number of particles in the excitation volume corresponds to the absolute concentration of the particles, whereas the brightness value provides a measure of the stoichiometry. For GFP fusions, if one knows the molecular brightness of monomeric GFP, then the ratio of the molecular brightness of the diffusing particles to that of monomeric GFP yields the stoichiometry of the diffusing particles. The brightness of monomeric GFP for the imaging conditions used was found to be 0.04 counts per 40 microseconds dwell-time per molecule. For fluctuations to be observed, the fluorescent

particle of interest must diffuse on the seconds timescale, corresponding to the frame time. Hence even large slowly diffusing particles can be investigated, provided they move on this rather slow timescale.

Expression of the Ty1 Gag-GFP construct was highly heterogeneous from cell to cell (Fig. 4A and 4B), which is consistent with prior reports that Gag and Gag-mRNA foci are present in only approximately 25–30% of cells [46, 49]. This heterogeneity was evident not only in the average intensity map (Fig. 4A left image), but also in both the Numbers and molecular Brightness maps (Fig. 4A middle and right images). Cells exhibiting low intensity also exhibited low number and brightness (red arrow), whereas high brightness correlated with high number (white arrow) (Fig. 4A). The true brightness for the cell indicated by the red arrow (0.036) corresponded to that of monomeric GFP, but some true brightness values reached 100-fold that of monomeric GFP. These large brightness values corresponded to diffusing foci of varying sizes (up to 1–2 microns in diameter) (see Movie 1).

Gag-GFP concentration was determined in young mother cells and buds from unsorted populations and from duplicate populations of aged mother cells (average age 7.9 ± 0.8) and their daughter cells. The histogram of concentrations in these cells highlights the heterogeneity noted in the images (Fig. 4B). Young mothers had a significant 2-fold reduction in cells in the lowest concentration bin and 3.4-fold increase in the second highest bin compared to buds, but a 2-fold increase in the highest concentration bin was not significant (Fig. 4B). Aged mothers exhibited even greater heterogeneity, with significant 2.6-fold and 2.2-fold increases in cells in the lowest and highest concentration bins, respectively, compared to their daughter cells, and fewer cells in the medium concentration bins (Fig. 4B). The daughter cell populations from the aged mothers are a mixture of newborn daughters and young mothers, and this was reflected in their distribution between the concentration bins (Fig. 4B). Aged mother populations had a greater proportion of cells in the highest concentration bin than young mothers, but this difference was not quite significant. Overall, mother cells had greater proportions of cells with very high concentrations of Gag-GFP with a trend for the proportion to increase with age for the highest concentrations. Cells with these very high concentrations have large Gag-GFP foci (Movie 1). Therefore, aging mother cells may accumulate Gag-mRNA complexes and VLPs, limiting their inheritance by daughter cells, which would contribute to high Ty1 mobility in aging mother cells.

3.5 Aging mother cells accumulate higher Ty1 cDNA levels than their daughter cells

Unincorporated Ty1 cDNA was quantified through an established Southern blot assay using DNA extracts of mother and daughter cells to further test whether differential regulation of Ty1 replication underlies the difference in retromobility between mother and daughter cells [36]. Cells were grown as for prior experiments, and restriction enzyme digested DNA was hybridized with a probe to the 3′ end of Ty1. The 3′ cDNA fragment has no flanking genomic sequence, so it migrates faster than the 3′ fragment of genomic copies of Ty1 and can be quantified relative to the genomic Ty1 fragments (Figs. 5A and 5B). Wild type mother cells 3.9, 11, and 17 generations old had 3.4, 9.4, and 12-fold higher cDNA levels than their daughter cells, respectively (Fig. 5C). The difference for the youngest mother cell

populations was not significant because of variability in cDNA levels at this point, which could indicate that cDNA does not consistently accumulate to high levels until cells have undergone several rounds of cell division at permissive temperature (or could result from the slightly lower purity of the youngest mother cells, Fig. 5C). Old mother cells had much higher cDNA levels than the control unsorted populations (Fig. 5C). The differences in cDNA levels could account for the higher mobility in mothers compared to daughter cells and supports the speculation that the decline in Ty1 mobility in the oldest mothers results from failure of many old mother cells to divide (Fig. 1C), as opposed to a decline in Ty1 activity.

4. Discussion

Levels of Ty1 mobility observed in aging yeast mother cells and their daughter cells are consistent with preferential Ty1 insertions in mother cell genomes during cell division. If new insertions occur in mother cells prior to DNA replication and cell division, then subsequent daughter cells would inherit the new insertions. This would lead to similar mobility frequencies in mothers and daughters as cells continued to divide during replicative aging (Fig. 6A). If Ty1 retromobility occurs during DNA replication or cell division, then a new Ty1 insertion would be present in either the mother or daughter cell (but not both) after completion of cell division (Fig. 6B and 6C). If during cell division new Ty1 insertions were equally likely to occur in either the mother or daughter cell genome, then at a population level this would result in similar Ty1 mobility frequencies in mother and daughter cells (Fig. 6B). If the new Ty1 insertions occurred preferentially in the mother cell genomes during division, then mother cells would have higher Ty1 mobility frequencies than their daughter cells (Fig. 6C). Since aging mother cells had higher Ty1 mobility than their daughters, new insertions appear to preferentially occur in mothers during cell cycle progression (Fig. 6C). In this model, the asymmetry would only occur between mothers and newborn daughters. Once newborn daughters become young mothers, they would have a chance to acquire Ty1 integration events.

Importantly, elevated Ty1 retromobility in the youngest mothers examined compared to their daughters implies that functional decline associated with advanced age is not required for retrotransposition to be elevated in mother cells. Rather, a mother-cell or age-specific mechanism causing accumulation of Gag complexes and cDNA in mother cells may lead to accumulation of insertions as replicative age increases. A recent study noted that Ty1 mRNA levels were much higher in old mother cells than young daughter cells [6]. A modest increase in Ty1*HIS3* mRNA for aged mothers compared to their daughters was noted in the current study, but aged mothers did not have more Ty1*HIS3* mRNA than unsorted young populations. This difference compared to the prior study could potentially result from aging cells at 20°C in the current study or differences in accumulation of RNA from the marked element compared to other genomic copies of Ty1, but will require further investigation.

The results presented here extend a previously reported observation that foci of Ty1 mRNA and Gag protein are enriched in budding cells compared to cells that are not dividing [46]. These foci are thought to represent precursors to VLPs [46, 50]. Young mothers were more likely to have high Gag-GFP concentrations than buds, and the proportion of cells with the

highest concentrations of Gag-GFP further increased in aged mothers (Fig. 4B). Cells with very high Gag-GFP concentrations contained large foci, but further work will be required to determine if these are VLPs. Ty1 mobility is inhibited in G1-arrested cells but not G2-arrested cells, indicating that Ty1 replication is linked to progression through the cell cycle [51]. An interesting possibility based on these observations is that VLPs form or are retained in mother cells during cell division, leading to the greater levels of Ty1 cDNA and retromobility observed in aging mothers.

Ty1 retromobility, multimeric insertions, and GCRs showed a similar trend of increasing with replicative age, but then declined in the oldest mothers examined. However, high cDNA levels in the oldest mothers are consistent with high Ty1 activity. If the mother cells accumulating Ty1 insertions associated with GCRs were also the cells that lost reproductive capacity earlier, then this could result in an apparent decrease in new Ty1 insertions and genome instability in the oldest mother cells. This would not necessarily mean that the Ty1 insertions were responsible for the loss of reproductive capacity, but the possibility that Ty1 insertions in mother cells could promote genome instability that causes cells to cease dividing warrants further investigation. The RNA polymerase III subunit AC40p encoded by the *RPC40* gene was recently shown to have a major role in directing Ty1 insertions to sites upstream of tRNA genes [52]. A modest reduction in *RPC40* expression during replicative aging [53] could have resulted in the detection of a telomeric insertion in aged mothers, but would not account for the multiple insertions into *RDN25* in the rDNA [52]. The identification of higher than expected numbers of Ty1 insertions into preferred and non-preferred sites in the rDNA in mother cells is noteworthy, since the rDNA region is prone to recombination and translocation events during replicative aging [6, 54], raising the possibility that Ty1 insertions could contribute to these events.

Several studies that identified increased retrotransposition with age by measuring copy number changes detected by qPCR found the increases to be associated with reduced chromatin-mediated silencing with age [3, 4, 6, 7]. For example, increased L1 retrotransposon expression in senescent human cells and in somatic tissues of aged mice was recently correlated to loss with age of SIRT6 binding to the L1 5′ untranslated region [7]. While the results reported here do not conflict with these prior studies, they raise the possibility that additional mechanisms beyond loss of normal silencing could regulate retrotransposition during aging. Interestingly, an earlier study found that retrotransposition of a plasmid copy of a human L1 retrotransposon expressed from its endogenous promoter occurred at high levels in proliferating normal human fibroblasts, but at lower levels as cells approached senescence [20]. Levels of retrotransposition with age may be influenced by a combination of mechanisms dependent on cellular proliferation and mechanisms that change with advanced age. The identification of high levels of unincorporated Ty1 cDNA in the current study, which would contribute to qPCR-based copy number measurements, also highlights the importance of directly measuring retrotransposition in future studies of age-dependent regulation.

Overall, this work provides a new perspective for evaluating the emerging associations of retrotransposons with aging that have been identified in multiple species, by providing support for a regulatory mechanism acting earlier than expected during replicative aging.

Supplementary Material

Refer to Web version on PubMed Central for supplementary material.

Acknowledgments

The authors would like to thank Joan Curcio for providing strains JC3212 and JC3807, David VanHoute for comments on the manuscript and helpful discussions, and John Hayes and Michelle Gruttadauria for technical assistance. This work was supported in part by grant R00AG031911 from the National Institute on Aging to P. H. M. Content of this article does not necessarily represent official views of the National Institutes of Health.

Abbreviations

ddPCR	droplet digital PCR
GCR	gross chromosomal rearrangement
LTR	long terminal repeat
MSS	Ma-Sandri-Sarkar
N&B	two-photon scanning Number & Brightness
ORF	open reading frame
qPCR	quantitative PCR
VLP	virus-like particle
WGA	wheat germ agglutinin

References

1. Beauregard A, Curcio MJ, Belfort M. The take and give between retrotransposable elements and their hosts. Annu Rev Genet. 2008; 42:587–617. [PubMed: 18680436]
2. Dennis S, Sheth U, Feldman JL, English KA, Priess JR. C. elegans germ cells show temperature and age-dependent expression of Cer1, a Gypsy/Ty3-related retrotransposon. PLoS Pathog. 2012; 8:e1002591. [PubMed: 22479180]
3. De Cecco M, Criscione SW, Peckham EJ, Hillenmeyer S, Hamm EA, Manivannan J, Peterson AL, Kreiling JA, Neretti N, Sedivy JM. Genomes of replicatively senescent cells undergo global epigenetic changes leading to gene silencing and activation of transposable elements. Aging Cell. 2013; 12:247–256. [PubMed: 23360310]
4. De Cecco M, Criscione SW, Peterson AL, Neretti N, Sedivy JM, Kreiling JA. Transposable elements become active and mobile in the genomes of aging mammalian somatic tissues. Aging (Albany NY). 2013; 5:867–883. [PubMed: 24323947]
5. Li W, Prazak L, Chatterjee N, Grüninger S, Krug L, Theodorou D, Dubnau J. Activation of transposable elements during aging and neuronal decline in Drosophila. Nat Neurosci. 2013; 16:529–531. [PubMed: 23563579]
6. Hu Z, Chen K, Xia Z, Chavez M, Pal S, Seol JH, Chen CC, Li W, Tyler JK. Nucleosome loss leads to global transcriptional up-regulation and genomic instability during yeast aging. Genes Dev. 2014; 28:396–408. [PubMed: 24532716]
7. Van Meter M, Kashyap M, Rezazadeh S, Geneva AJ, Morello TD, Seluanov A, Gorbunova V. SIRT6 represses LINE1 retrotransposons by ribosylating KAP1 but this repression fails with stress and age. Nat Commun. 2014; 5:5011. [PubMed: 25247314]
8. Maxwell PH, Burhans WC, Curcio MJ. Retrotransposition is associated with genome instability during chronological aging. Proc Natl Acad Sci U S A. 2011; 108:20376–20381. [PubMed: 22021441]

9. Umezu K, Hiraoka M, Mori M, Maki H. Structural analysis of aberrant chromosomes that occur spontaneously in diploid Saccharomyces cerevisiae: retrotransposon Ty1 plays a crucial role in chromosomal rearrangements. Genetics. 2002; 160:97–110. [PubMed: 11805048]
10. Maksakova IA, Romanish MT, Gagnier L, Dunn CA, van de Lagemaat LN, Mager DL. Retroviral elements and their hosts: insertional mutagenesis in the mouse germ line. PLoS Genet. 2006; 2:e2. [PubMed: 16440055]
11. Wallace NA, Belancio VP, Deininger PL. L1 mobile element expression causes multiple types of toxicity. Gene. 2008; 419:75–81. [PubMed: 18555620]
12. Beck CR, Garcia-Perez JL, Badge RM, Moran JV. LINE-1 elements in structural variation and disease. Annu Rev Genomics Hum Genet. 2011; 12:187–215. [PubMed: 21801021]
13. Huang CR, Burns KH, Boeke JD. Active transposition in genomes. Annu Rev Genet. 2012; 46:651–675. [PubMed: 23145912]
14. Robberecht C, Voet T, Esteki MZ, Nowakowska BA, Vermeesch JR. Nonallelic homologous recombination between retrotransposable elements is a driver of de novo unbalanced translocations. Genome Res. 2013; 23:411–418. [PubMed: 23212949]
15. Sedivy JM, Kreiling JA, Neretti N, De Cecco M, Criscione SW, Hofmann JW, Zhao X, Ito T, Peterson AL. Death by transposition - the enemy within? Bioessays. 2013; 35:1035–1043. [PubMed: 24129940]
16. Wood JG, Helfand SL. Chromatin structure and transposable elements in organismal aging. Front Genet. 2013; 4:274. [PubMed: 24363663]
17. Gorbunova V, Boeke JD, Helfand SL, Sedivy JM. Human Genomics. Sleeping dogs of the genome. Science. 2014; 346:1187–1188. [PubMed: 25477445]
18. Goodier JL. Retrotransposition in tumors and brains. Mob DNA. 2014; 5:11. [PubMed: 24708615]
19. Wang J, Geesman GJ, Hostikka SL, Atallah M, Blackwell B, Lee E, Cook PJ, Pasaniuc B, Shariat G, Halperin E, Dobke M, Rosenfeld MG, Jordan IK, Lunyak VV. Inhibition of activated pericentromeric SINE/Alu repeat transcription in senescent human adult stem cells reinstates self-renewal. Cell Cycle. 2011; 10:3016–3030. [PubMed: 21862875]
20. Shi X, Seluanov A, Gorbunova V. Cell divisions are required for L1 retrotransposition. Mol Cell Biol. 2007; 27:1264–1270. [PubMed: 17145770]
21. VanHoute D, Maxwell PH. Extension of Saccharomyces paradoxus chronological lifespan by retrotransposons in certain media conditions is associated with changes in reactive oxygen species. Genetics. 2014; 198:531–545. [PubMed: 25106655]
22. Longo VD, Shadel GS, Kaeberlein M, Kennedy B. Replicative and chronological aging in Saccharomyces cerevisiae. Cell Metab. 2012; 16:18–31. [PubMed: 22768836]
23. Lee BS, Lichtenstein CP, Faiola B, Rinckel LA, Wysock W, Curcio MJ, Garfinkel DJ. Posttranslational inhibition of Ty1 retrotransposition by nucleotide excision repair/transcription factor TFIIH subunits Ssl2p and Rad3p. Genetics. 1998; 148:1743–1761. [PubMed: 9560391]
24. Scholes DT, Banerjee M, Bowen B, Curcio MJ. Multiple regulators of Ty1 transposition in Saccharomyces cerevisiae have conserved roles in genome maintenance. Genetics. 2001; 159:1449–1465. [PubMed: 11779788]
25. Amberg, DC.; Burke, DJ.; Strathern, JN. Methods in Yeast Genetics: A Cold Spring Harbor Laboratory Course Manual. 2005. Cold Spring Harbor Laboratory Press; Cold Spring Harbor, New York: 2005.
26. Mou Z, Kenny AE, Curcio MJ. Hos2 and Set3 promote integration of Ty1 retrotransposons at tRNA genes in Saccharomyces cerevisiae. Genetics. 2006; 172:2157–2167. [PubMed: 16415356]
27. Scholes DT, Kenny AE, Gamache ER, Mou Z, Curcio MJ. Activation of a LTR-retrotransposon by telomere erosion. Proc Natl Acad Sci U S A. 2003; 100:15736–15741. [PubMed: 14673098]
28. Dutko JA, Kenny AE, Gamache ER, Curcio MJ. 5′ to 3′ mRNA decay factors colocalize with Ty1 gag and human APOBEC3G and promote Ty1 retrotransposition. J Virol. 2010; 84:5052–5066. [PubMed: 20219921]
29. Patterson MN, Maxwell PH. Combining Magnetic Sorting of Mother Cells and Fluctuation Tests to Analyze Genome Instability During Mitotic Cell Aging in Saccharomyces cerevisiae. J Vis Exp. 2014

30. Curcio MJ, Garfinkel DJ. Single-step selection for Ty1 element retrotransposition. Proc Natl Acad Sci U S A. 1991; 88:936–940. [PubMed: 1846969]
31. Foster PL. Methods for determining spontaneous mutation rates. Methods Enzymol. 2006; 409:195–213. [PubMed: 16793403]
32. Hall BM, Ma CX, Liang P, Singh KK. Fluctuation analysis CalculatOR: a web tool for the determination of mutation rate using Luria-Delbruck fluctuation analysis. Bioinformatics. 2009; 25:1564–1565. [PubMed: 19369502]
33. Siebert PD, Chenchik A, Kellogg DE, Lukyanov KA, Lukyanov SA. An improved PCR method for walking in uncloned genomic DNA. Nucleic Acids Res. 1995; 23:1087–1088. [PubMed: 7731798]
34. Maxwell PH, Curcio MJ. Retrosequence formation restructures the yeast genome. Genes Dev. 2007; 21:3308–3318. [PubMed: 18079177]
35. Digman MA, Dalal R, Horwitz AF, Gratton E. Mapping the number of molecules and brightness in the laser scanning microscope. Biophys J. 2008; 94:2320–2332. [PubMed: 18096627]
36. Lee BS, Bi L, Garfinkel DJ, Bailis AM. Nucleotide excision repair/TFIIH helicases RAD3 and SSL2 inhibit short-sequence recombination and Ty1 retrotransposition by similar mechanisms. Mol Cell Biol. 2000; 20:2436–2445. [PubMed: 10713167]
37. Smeal T, Claus J, Kennedy B, Cole F, Guarente L. Loss of transcriptional silencing causes sterility in old mother cells of S. cerevisiae. Cell. 1996; 84:633–642. [PubMed: 8598049]
38. Paquin CE, Williamson VM. Temperature effects on the rate of ty transposition. Science. 1984; 226:53–55. [PubMed: 17815421]
39. Lawler JF, Haeusser DP, Dull A, Boeke JD, Keeney JB. Ty1 defect in proteolysis at high temperature. J Virol. 2002; 76:4233–4240. [PubMed: 11932388]
40. Baller JA, Gao J, Stamenova R, Curcio MJ, Voytas DF. A nucleosomal surface defines an integration hotspot for the Saccharomyces cerevisiae Ty1 retrotransposon. Genome Res. 2012; 22:704–713. [PubMed: 22219511]
41. Mularoni L, Zhou Y, Bowen T, Gangadharan S, Wheelan SJ, Boeke JD. Retrotransposon Ty1 integration targets specifically positioned asymmetric nucleosomal DNA segments in tRNA hotspots. Genome Res. 2012; 22:693–703. [PubMed: 22219510]
42. Venema J, Tollervey D. Ribosome synthesis in Saccharomyces cerevisiae. Annu Rev Genet. 1999; 33:261–311. [PubMed: 10690410]
43. Bryk M, Banerjee M, Conte D, Curcio MJ. The Sgs1 helicase of Saccharomyces cerevisiae inhibits retrotransposition of Ty1 multimeric arrays. Mol Cell Biol. 2001; 21:5374–5388. [PubMed: 11463820]
44. Stamenova R, Maxwell PH, Kenny AE, Curcio MJ. Rrm3 protects the Saccharomyces cerevisiae genome from instability at nascent sites of retrotransposition. Genetics. 2009; 182:711–723. [PubMed: 19414561]
45. Sundararajan A, Lee BS, Garfinkel DJ. The Rad27 (Fen-1) nuclease inhibits Ty1 mobility in Saccharomyces cerevisiae. Genetics. 2003; 163:55–67. [PubMed: 12586696]
46. Checkley MA, Nagashima K, Lockett SJ, Nyswaner KM, Garfinkel DJ. P-body components are required for Ty1 retrotransposition during assembly of retrotransposition-competent virus-like particles. Mol Cell Biol. 2010; 30:382–398. [PubMed: 19901074]
47. Digman MA, Gratton E. Fluorescence correlation spectroscopy and fluorescence cross-correlation spectroscopy. Wiley Interdiscip Rev Syst Biol Med. 2009; 1:273–282. [PubMed: 20835996]
48. Moutin E, Compan V, Raynaud F, Clerté C, Bouquier N, Labesse G, Ferguson ML, Fagni L, Royer CA, Perroy J. The stoichiometry of scaffold complexes in living neurons - DLC2 functions as a dimerization engine for GKAP. J Cell Sci. 2014; 127:3451–3462. [PubMed: 24938595]
49. Malagon F, Jensen TH. The T body, a new cytoplasmic RNA granule in Saccharomyces cerevisiae. Mol Cell Biol. 2008; 28:6022–6032. [PubMed: 18678648]
50. Malagon F, Jensen TH. T-body formation precedes virus-like particle maturation in S. cerevisiae. RNA Biol. 2011; 8:184–189. [PubMed: 21358276]
51. Xu H, Boeke JD. Inhibition of Ty1 transposition by mating pheromones in Saccharomyces cerevisiae. Mol Cell Biol. 1991; 11:2736–2743. [PubMed: 1850102]

52. Bridier-Nahmias A, Tchalikian-Cosson A, Baller JA, Menouni R, Fayol H, Flores A, Saïb A, Werner M, Voytas DF, Lesage P. Retrotransposons. An RNA polymerase III subunit determines sites of retrotransposon integration. Science. 2015; 348:585–588. [PubMed: 25931562]

53. Yiu G, McCord A, Wise A, Jindal R, Hardee J, Kuo A, Shimogawa MY, Cahoon L, Wu M, Kloke J, Hardin J, Mays Hoopes LL. Pathways change in expression during replicative aging in Saccharomyces cerevisiae. J Gerontol A Biol Sci Med Sci. 2008; 63:21–34. [PubMed: 18245757]

54. Lindstrom DL, Leverich CK, Henderson KA, Gottschling DE. Replicative age induces mitotic recombination in the ribosomal RNA gene cluster of Saccharomyces cerevisiae. PLoS Genet. 2011; 7:e1002015. [PubMed: 21436897]

Highlights

- Ty1 retrotransposition is more frequent in yeast mothers than their daughter cells
- Ty1 mobility exceeds age-based predictions and is associated with genome instability
- Mother cells have higher Ty1 Gag protein concentrations than daughter cells
- Aging mother cells have more Ty1 reverse transcripts (cDNA) than their daughter cells
- Age-dependent Ty1 regulation begins early during yeast replicative lifespan

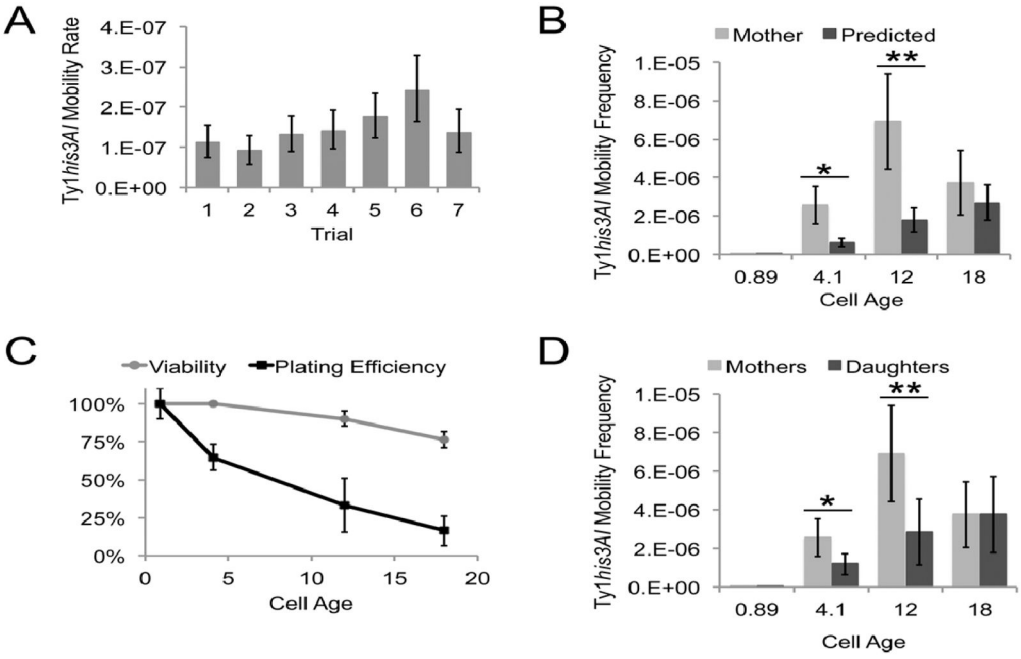

Fig. 1. Aging yeast mother cells have higher levels of Ty1 retromobility than predicted

(A) The rates per cell generation and 95% confidence intervals for Ty1*his3AI* mobility calculated using the MSS maximum likelihood method for seven independent trials using unsorted cultures are shown. (B) The means and standard deviations of Ty1*his3AI* mobility from six experiments for mother cells that underwent the indicated numbers of cell generations (light gray columns) are compared to the mean predicted frequencies and 95% confidence intervals for cells of the indicated ages (dark gray columns). (C) Means and standard deviations for viability measured by trypan blue dye exclusion and for normalized plating efficiencies based on colony-forming units for cells of the indicated ages from five experiments are shown. (D) The same Ty1*his3AI* mobility data for mother cells from (B) (light gray columns) are compared to the means and standard deviations of Ty1*his3AI* mobility in the corresponding daughter cell populations (dark gray columns). Symbols * and ** indicate $p < 0.05$ and $p < 0.01$, respectively.

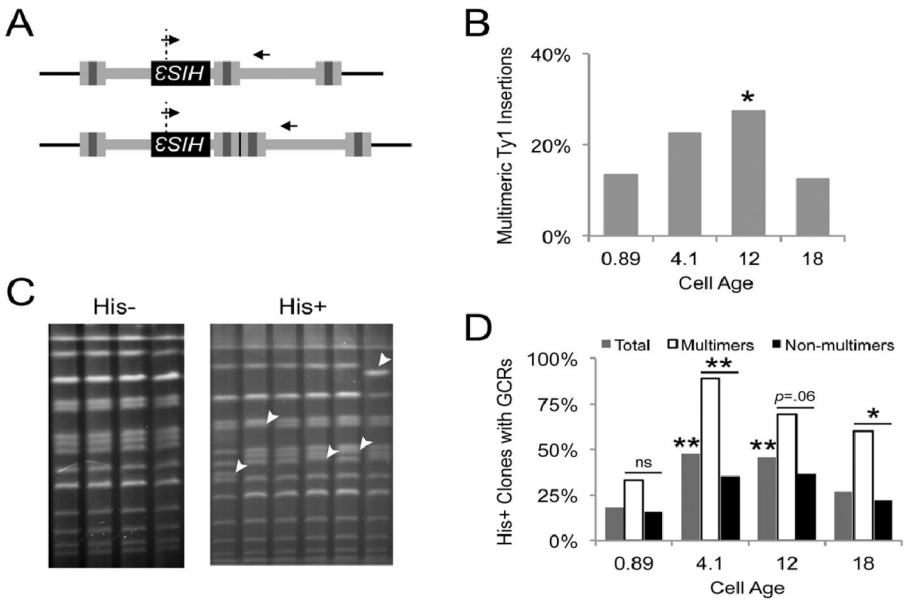

Fig. 2. Ty1 insertions are correlated with gross chromosome rearrangements (GCRs) in aging yeast mother cells

(A) Illustrations (not to scale) of multimeric Ty1 insertions in which tandem copies of Ty1 share an LTR (tripartite gray box) or in which each element has two distinct LTRs (top and bottom images, respectively). A dotted line indicates the position of the splice junction in *HIS3* and small arrows indicate the relative positions of PCR primers. (B) Percent of Ty1*HIS3* insertions identified as multimeric using the PCR strategy shown in (A) for unsorted cell populations (age 0.89) or mother cells of the indicated ages (n = 111, 40, 51, and 80 for each age group, respectively). (C) Representative pulse-field gel images of intact chromosomes visualized with ethidium bromide for four clones lacking a Ty1*HIS3* insertion (His^-) and six clones harboring a Ty1*HIS3* insertion (His^+) obtained after one round of growth and sorting. White arrowheads point to chromosome bands that have shifted to new positions. (D) Percent of clones with Ty1*HIS3* insertions harboring a GCR (gray columns) for unsorted cell populations (age 0.89) and mother cell populations of the indicated ages (n = 104, 40, 46, and 82 for each age group, respectively). Percent of cells for each age with multimeric Ty1*HIS3* insertions that also harbored a GCR (white columns) are compared to the percent of cells for each age with non-multimeric insertions that harbored a GCR (black columns). Significant differences are indicated for percent of total clones with GCRs in mother cells compared to the unsorted cell populations, and for clones with multimers compared to clones without multimers in each age category. Symbols * and ** indicate $p < 0.05$ and $p < 0.01$, respectively.

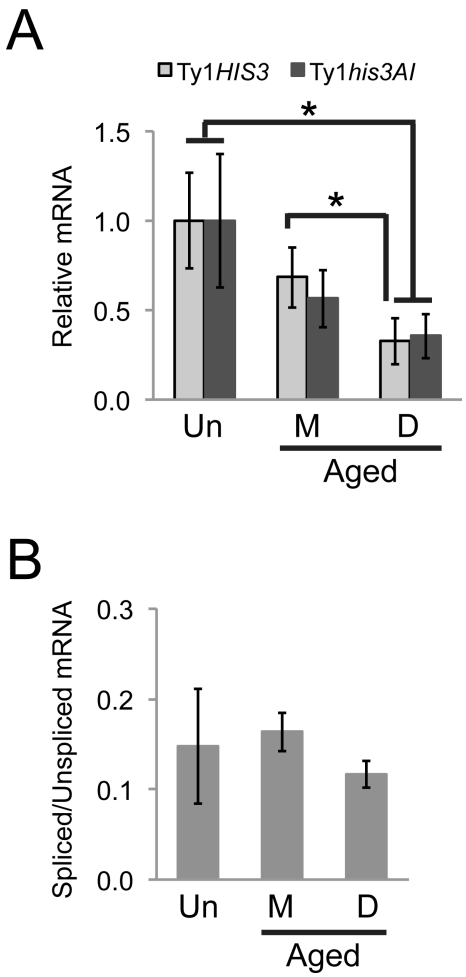

Fig. 3. Aged mother cells have more Ty1*HIS3* mRNA than their daughters, but not more than young cell populations

(A) Ty1*HIS3* and Ty1*his3AI* mRNA levels measured through ddPCR of reverse-transcribed RNA from duplicate young unsorted populations (Un), four aged mother cell populations (M), and their four daughter cell populations (D) were normalized to *ACT1* mRNA levels and are shown relative to the average level in the unsorted populations. Average ages of the four mother cell populations were 7.7, 8.3, 16, and 19. Average purity of these mother cell populations was 98 ± 1.0%. Symbol * indicates $p < 0.05$. (B) Ratio of the spliced Ty1*HIS3* mRNA to the unspliced Ty1*his3AI* mRNA for the samples from panel (A).

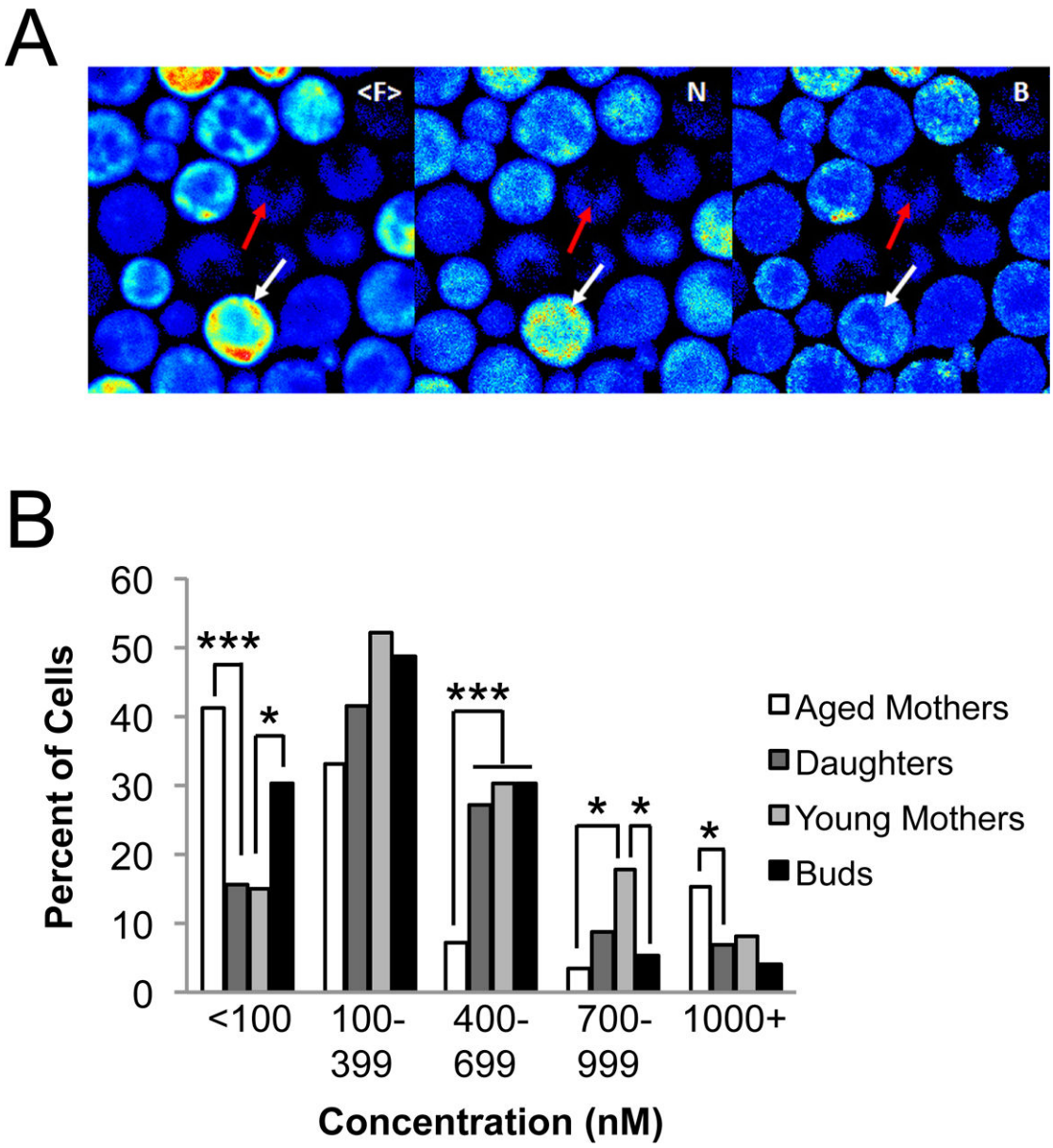

Fig. 4. Greater proportions of mother cell populations have very high concentrations of Ty1 Gag-GFP than daughter cell populations

(A) Representative images from two photon scanning N&B analysis with the strain expressing Ty1 Gag-GFP. Left image is the average fluorescence intensity from 50 raster scans, middle image is the Numbers map (not shot noise corrected), and right image is the Brightness map (also not shot noise corrected). Full scale <F> 0–9.8, N – 0–6.0, B – 0–8.9. Red arrows indicate a cell with low levels of Gag-GFP, whereas the white arrows indicate a cell with higher levels (warm colors indicate higher signal). Each image is 20 × 20 μm. (B) Absolute concentrations (nM) of Gag-GFP measured by two photon scanning N&B analysis for cells from duplicate aged mother populations (average age 7.9), their daughter cell populations, and duplicate unsorted young cell populations (young mothers and buds). A total of 85, 147, 90, and 90 cells were analyzed for aged mothers, their daughter populations,

young mothers, and buds, respectively. Symbols * and *** indicate $p < 0.05$ and $p < 0.001$, respectively.

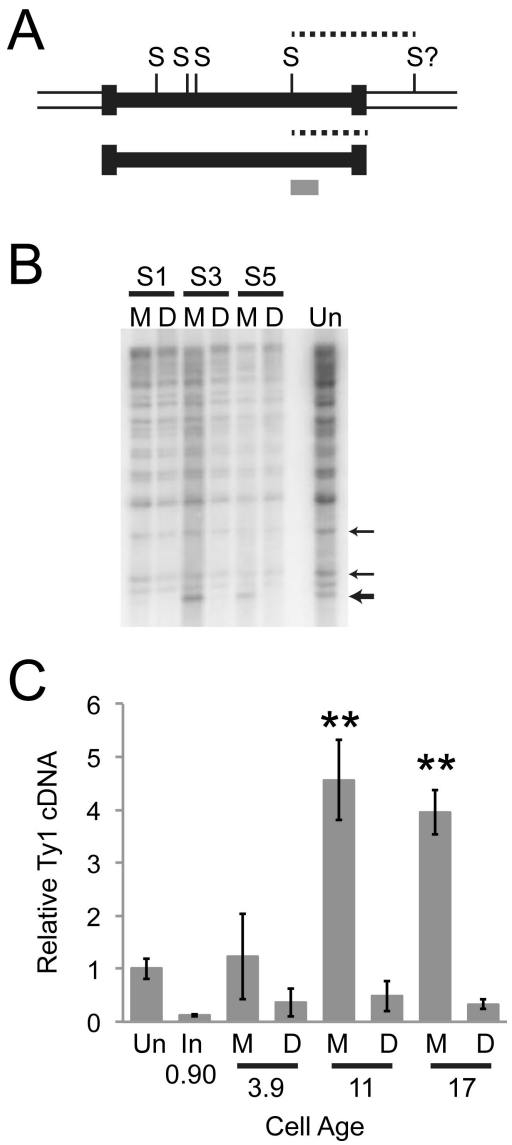

Fig. 5. Preferential accumulation of Ty1 cDNA in old mother cells

(A) Illustration of a genomic Ty1 and unincorporated Ty1 cDNA (black boxes) indicating sites for the restriction enzyme SphI (S) and corresponding position of the radiolabeled DNA probe (gray box). Dotted lines indicate restriction fragments detected by the probe, which are variable for genomic copies of Ty1, due to the distance to the next SphI site (S?). (B) Example Southern blot of DNA from unsorted cells (Un) or mother (M) and daughter (D) cell populations obtained after one, three, or five rounds of growth and sorting (S1, S3, or S5, respectively). Larger arrow indicates the position of the cDNA fragment and smaller arrows indicate positions of genomic Ty1 fragments used to normalize the cDNA signal. (C) Means and standard deviations of cDNA levels normalized to those in unsorted cell populations grown at permissive temperature (20°C, Un), for initial cell populations grown at non-permissive temperature (30°C, In), and for mother cells of the indicated cell ages grown at permissive temperature (M) and their daughter cell populations (D). Average purity of mother cells was 75 ± 7.9%, 97 ± 1.4%, and 98 ± 1% for the youngest to oldest

mothers, respectively (mean and standard deviation). The symbol ** indicates $p < 0.01$ for mothers compared to their daughters.

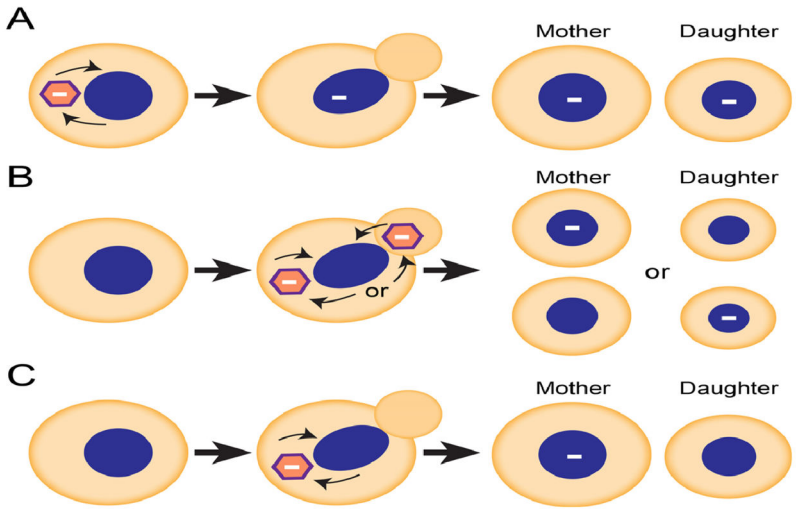

Fig. 6. Proposed model for accumulation of Ty1 insertions in aging mother cells

Three alternative models are shown to represent how the timing of Ty1 replication in regards to cell division could result in different outcomes for retromobility frequencies in mothers and daughters. Blue circles/ellipses represent nuclei, hexagons represent Ty1 VLPs, and white lines indicate Ty1 cDNA (in VLPs) or new Ty1 integration events (in nuclei). (A) If new Ty1 insertions predominantly occur in non-dividing cells, mother cells would pass any new insertions to daughters and mothers and daughters should have similar Ty1 mobility frequencies. (B) If Ty1 insertions predominantly occur during or after S-phase when two genomes are present, but are equally likely to occur in the mother or bud genome ("or"), mothers or daughters have an equal chance of acquiring the new Ty1 insertion. This would again result in similar mobility frequencies in mothers and daughters. (C) If Ty1 insertions predominantly occur during or after S phase but preferentially occur in mother cells genomes, mother cells will acquire new insertions that are absent from their daughter cells. This would result in higher Ty1 mobility in mother cells, and this model is most consistent with the data presented.

Table 1

Ty1 insertions at non-preferred genomic target sites in aging mother cells.

		<2 kb from RNA pol III- transcribed gene				Non-preferred targets[d]	
Mean Mother Cell Age	**N**	**tRNA gene**	***RDN5*[a]**	***SNR6*[b]**	**<500 bp from ORF[c]**	***RDN25*[e]**	**Telomere[f]**
4.1	22	18	2	0	0	1	1
12	27	22	3	1	1	2	0
18	26	20	3	0	1	0	0

[a] 5S rRNA gene

[b] U6 spliceosomal RNA gene

[c] Sites near an ORF but not also near a RNA pol III transcribed gene

[d] Genomic sites not previously found to be frequent sites of Ty1 insertions

[e] Within transcribed portion of 25S rRNA gene

[f] Between a Y′ element and X element